

# Relativistic jet activity from the tidal disruption of a star by a massive black hole

D. N. Burrows<sup>1</sup>, J. A. Kennea<sup>1</sup>, G. Ghisellini<sup>2</sup>, V. Mangano<sup>3</sup>, B. Zhang<sup>4</sup>, K. L. Page<sup>5</sup>, M. Eracleous<sup>1</sup>, P. Romano<sup>3</sup>, T. Sakamoto<sup>6,7,8</sup>, A. D. Falcone<sup>1</sup>, J. P. Osborne<sup>5</sup>, S. Campana<sup>2</sup>, A. P. Beardmore<sup>5</sup>, A. A. Breeveld<sup>9</sup>, M. M. Chester<sup>1</sup>, R. Corbet<sup>6,7,8</sup>, S. Covino<sup>2</sup>, J. R. Cummings<sup>6,7,8</sup>, P. D'Avanzo<sup>2</sup>, V. D'Elia<sup>10</sup>, P. Esposito<sup>11</sup>, P. A. Evans<sup>5</sup>, D. Fugazza<sup>2</sup>, J. M. Gelbord<sup>1</sup>, K. Hiroi<sup>12</sup>, S. T. Holland<sup>6,7,13</sup>, K. Y. Huang<sup>14</sup>, M. Im<sup>15</sup>, G. Israel<sup>16</sup>, Y. Jeon<sup>15</sup>, Y.-B. Jeon<sup>17</sup>, H. D. Jun<sup>15</sup>, N. Kawai<sup>18,19</sup>, J. H. Kim<sup>15</sup>, H. A. Krimm<sup>6,7,13</sup>, F. E. Marshall<sup>7</sup>, P. Mészáros<sup>1</sup>, H. Negoro<sup>20</sup>, N. Omodei<sup>21,22</sup>, W.-K. Park<sup>15</sup>, J. S. Perkins<sup>6,7,8</sup>, M. Sugizaki<sup>19</sup>, H.-I. Sung<sup>17</sup>, G. Tagliaferri<sup>2</sup>, E. Troja<sup>7</sup>, Y. Ueda<sup>12</sup>, Y. Urata<sup>23</sup>, R. Usui<sup>18</sup>, L. A. Antonelli<sup>10,16</sup>, S. D. Barthelmy<sup>7</sup>, G. Cusumano<sup>3</sup>, P. Giommi<sup>10</sup>, A. Melandri<sup>2</sup>, M. Perri<sup>10</sup>, J. L. Racusin<sup>7</sup>, B. Sbarufatti<sup>3</sup>, M. H. Siegel<sup>7</sup> & N. Gehrels<sup>7</sup>

Supermassive black holes have powerful gravitational fields with strong gradients that can destroy stars that get too close<sup>1,2</sup>, producing a bright flare in ultraviolet and X-ray spectral regions from stellar debris that forms an accretion disk around the black hole<sup>3-7</sup>. The aftermath of this process may have been seen several times over the past two decades in the form of sparsely sampled, slowly fading emission from distant galaxies<sup>8-14</sup>, but the onset of the stellar disruption event has not hitherto been observed. Here we report observations of a bright X-ray flare from the extragalactic transient Swift J164449.3+573451. This source increased in brightness in the X-ray band by a factor of at least 10,000 since 1990 and by a factor of at least 100 since early 2010. We conclude that we have captured the onset of relativistic jet activity from a supermassive black hole. A companion paper<sup>15</sup> comes to similar conclusions on the basis of radio observations. This event is probably due to the tidal disruption of a star falling into a supermassive black hole, but the detailed behaviour differs from current theoretical models of such events.

Swift J164449.3+573451 was discovered when it triggered the Swift<sup>16</sup> Burst Alert Telescope<sup>17</sup> (BAT) on 28 March 2011. Subsequent analysis of BAT data taken before the on-board trigger shows that the outburst was first detected on 25 March 2011 (Supplementary Fig. 1). The Swift X-Ray Telescope<sup>18</sup> (XRT) measured a source position<sup>19,20</sup> of right ascension (J2000) 16 h 44 min 49.92 s, declination (J2000) +57° 35' 00.6", with a 90% confidence error circle radius of 1.4 arcsec. Subsequent optical<sup>21</sup> and radio<sup>15</sup> observations showed that a variable radio source was located at the centre of a galaxy within the XRT error circle. Optical spectroscopy<sup>21</sup> measured a redshift of 0.354, corresponding to a luminosity distance  $D$  of  $5.8 \times 10^{27}$  cm (calculated as  $L = 4\pi D^2 F$ , where  $L$  is luminosity and  $F$  is flux).

We performed broad-band follow-up observations using  $\gamma$ -ray, X-ray, ultraviolet, optical and near-IR (NIR) telescopes. The flares seen by the BAT are closely tracked with better sensitivity in the 0.3–10-keV band by the XRT (Fig. 1). The X-ray light curve is complex and highly variable, with peak isotropic luminosities exceeding  $10^{48}$  erg s<sup>-1</sup> (Fig. 2), implying accretion onto a compact object. The integrated isotropic X-ray power (over the 50 days following the first BAT trigger)

is  $\sim 2 \times 10^{53}$  erg (1–10 keV). We have found no statistically significant periodic or quasi-periodic signals in the XRT data. Details of our observations and data analysis are given in Supplementary Information section 1.

Swift J164449.3+573451 has not been previously detected at any wavelength and is not present in any sky catalogues. X-ray flux upper limits from observations by ROSAT, XMM-Newton, MAXI and Swift between 1990 and 24 March 2011 are 2–4 orders of magnitude lower than the peak X-ray fluxes measured by Swift (Fig. 2), and the ROSAT upper limits are an order of magnitude below the lowest flux in the first 50 days after the first BAT trigger.

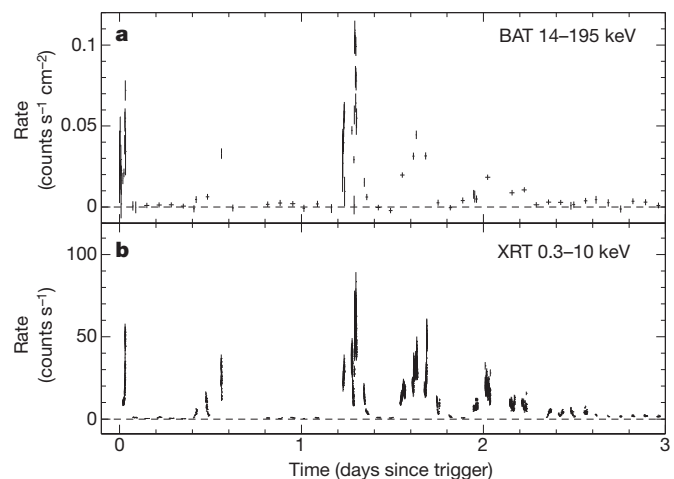


**Figure 1** | Swift BAT and XRT light curves for the first three days of observations. **a**, BAT light curve (14–195 keV). **b**, XRT light curve (0.3–10 keV). The horizontal axis is time in days since the first BAT on-board trigger on 28 March 2011. The BAT and XRT count rates track each other closely, with episodes of bright flaring (up to 200 mCrab in the BAT) in the first few days after the first BAT trigger. The source brightness then dropped dramatically, with an average BAT count rate of  $0.0020 \pm 0.0005$  counts cm<sup>-2</sup> s<sup>-1</sup> between 2 and 18 April 2011. Data gaps are caused by times when the source was not being observed. Error bars,  $1\sigma$ .

<sup>1</sup>Department of Astronomy and Astrophysics, The Pennsylvania State University, 525 Davey Laboratory, University Park, Pennsylvania 16802, USA. <sup>2</sup>INAF – Osservatorio Astronomico di Brera, Via Biancamano 46, 23807 Merate, Italy. <sup>3</sup>INAF – Istituto di Astrofisica Spaziale e Fisica Cosmica, Via U. La Malfa 153, I-90146 Palermo, Italy. <sup>4</sup>Department of Physics and Astronomy, University of Nevada, Las Vegas, Nevada 89154, USA. <sup>5</sup>Department of Physics and Astronomy, University of Leicester, University Road, Leicester LE1 7RH, UK. <sup>6</sup>CRESST, Greenbelt, Maryland 20771, USA. <sup>7</sup>NASA Goddard Space Flight Center, Greenbelt, Maryland 20771, USA. <sup>8</sup>University of Maryland, Baltimore County, 1000 Hilltop Circle, Baltimore, Maryland 21250, USA. <sup>9</sup>University College London / Mullard Space Science Laboratory, Holmbury St Mary, Dorking RH5 6NT, UK. <sup>10</sup>ASI Science Data Center, via Galileo Galilei, 00044 Frascati, Italy. <sup>11</sup>INAF – Osservatorio Astronomico di Cagliari, località Poggio dei Pini, strada 54, I-09012 Capoterra, Italy. <sup>12</sup>Department of Astronomy, Kyoto University, Oiwake-cho, Sakyo-ku, Kyoto 606-8502, Japan. <sup>13</sup>Universities Space Research Association, 10211 Wincopin Circle, Suite 500, Columbia, Maryland 21044-3432, USA. <sup>14</sup>Academia Sinica Institute of Astronomy and Astrophysics, Taipei 106, Taiwan. <sup>15</sup>Center for the Exploration of the Origin of the Universe, Department of Physics and Astronomy, FPRD, Seoul National University, Shillim-dong, San 56-1, Kwanak-gu, Seoul, Republic of Korea. <sup>16</sup>INAF – Osservatorio Astronomico di Roma, via Frascati 33, I-00040 Monteporzio Catone, Italy. <sup>17</sup>Korea Astronomy and Space Science Institute (KASI), 776 Daedeokdae-ro, Yuseong-gu, Daejeon 305-348, Republic of Korea. <sup>18</sup>Department of Physics, Tokyo Institute of Technology, 2-12-1 Ookayama, Meguro-ku, Tokyo 152-8551, Japan. <sup>19</sup>MAXI team, RIKEN, 2-1 Hirosawa, Wako, Saitama 351-0198, Japan. <sup>20</sup>Department of Physics, Nihon University, 1-8-14 Kanda-Surugadai, Chiyoda-ku, Tokyo 101-8308, Japan. <sup>21</sup>W. W. Hansen Experimental Physics Laboratory, Kavli Institute for Particle Astrophysics and Cosmology, Department of Physics, Stanford University, Stanford, California 94305, USA. <sup>22</sup>SLAC National Accelerator Laboratory, Stanford University, Stanford, California 94305, USA. <sup>23</sup>Institute of Astronomy, National Central University, Chung-Li 32054, Taiwan.

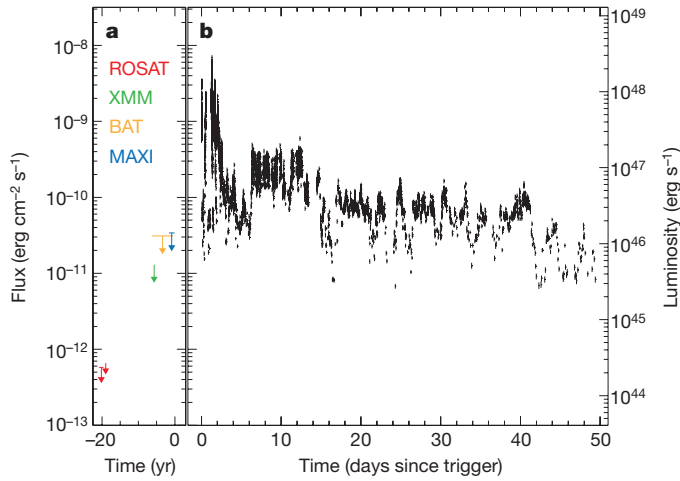


**Figure 2** | Swift XRT light curve of Swift J164449.3+573451 for the first 7 weeks of observations. **a**, Historical  $3\sigma$  X-ray flux upper limits from the direction of Swift J164449.3+573451, obtained by sky monitors and serendipitous observations over the past 20 years. The time axis for this panel is in years before the BAT on-board trigger on 28 March 2011. The horizontal bars on each upper limit indicate the time interval over which they were calculated, and are placed at the value of the  $3\sigma$  upper limit. All flux limits are calculated for the 1–10 keV band. (The BAT upper limit measured in its native energy band is about three orders of magnitude lower than the peak flux measured by the BAT during the early flares). **b**, XRT light curve in the 1–10 keV band. The X-ray events were summed into time bins containing 200 counts per bin and count rates were calculated for each time bin. Time-dependent spectral fits were used to convert count rates to absorption-corrected fluxes in the 1–10 keV band. The right-hand axis gives the conversion to luminosity of the source, assuming isotropic radiation and using  $H_0 = 71 \text{ km s}^{-1}$ ,  $\Omega_m = 0.27$  and  $\Omega_\Lambda = 0.73$ . Following nearly 3 days of intense flaring with peak fluxes over  $10^{-9} \text{ erg cm}^{-2} \text{ s}^{-1}$  and isotropic luminosities of  $\sim 10^{48} \text{ erg s}^{-1}$ , Swift J164449.3+573451 decayed over several days to a flux of about  $5 \times 10^{-11} \text{ erg cm}^{-2} \text{ s}^{-1}$ , then rose rapidly to  $\sim 2 \times 10^{-10} \text{ erg cm}^{-2} \text{ s}^{-1}$  for about a week. It has been gradually fading since. Details of the upper limits and XRT light curve are given in Supplementary Information section 1. Vertical error bars,  $1\sigma$ . Time bin widths are smaller than the line width of the vertical error bars.

Swift J164449.3+573451 is unlike any previously discovered extragalactic X-ray transient.  $\gamma$ -ray bursts reach similar peak fluxes and luminosities, but fade much more rapidly and smoothly than Swift J164449.3+573451. The broad class of active galactic nuclei cover the range of luminosities that we measured for Swift J164449.3+573451 ( $3 \times 10^{45}$  to  $3 \times 10^{48} \text{ erg s}^{-1}$ ), but no individual active galactic nucleus has been observed to vary by more than about two orders of magnitude. Supernovae have much lower luminosities (X-ray luminosity  $L_X < 3 \times 10^{41} \text{ erg s}^{-1}$ ). Some Galactic transients (such as supergiant fast X-ray transients) vary by similar amounts<sup>22</sup>, but their luminosities are 10 orders of magnitude lower than that of Swift J164449.3+573451. This source appears to be without precedent in its high energy properties.

Our X-ray and NIR observations provide limits on the mass of the accreting black hole. The most rapid observed variability is a  $3\sigma$  doubling in X-ray brightness over a timescale of  $\delta t_{\text{obs}} \approx 100 \text{ s}$ . This constrains the size of the black hole under the assumption that the central engine dominates the variability. For a Schwarzschild black hole with mass  $M_{\text{bh}}$  and radius  $r_s$ , the minimum variability timescale in its rest frame is  $\delta t_{\text{min}} \approx r_s/c \approx 10.0(M_6) \text{ s}$ , where  $M_6 \equiv (M_{\text{bh}}/10^6 M_\odot)$  and  $M_\odot$  is the solar mass. At  $z = 0.354$ , this gives:

$$M_{\text{bh}} \approx 7.4 \times 10^6 \left( \frac{\delta t_{\text{obs}}}{100} \right) M_\odot \quad (1)$$

where  $\delta t_{\text{obs}}$  is in seconds. Much smaller masses are unlikely, as they would lead to shorter timescale variability. However, short timescale

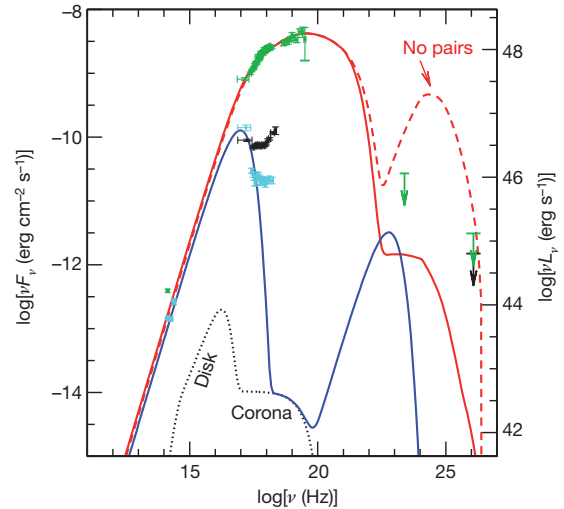


**Figure 3** | The spectral energy distribution of Swift J164449.3+573451. The green data points (and upper limits) are from the early bright flaring phase; cyan data points are from the low state at 4.5 days; black data points (and upper limit) are from roughly 8 days after the first BAT trigger. Error bars,  $1\sigma$ . The NIR fluxes were dereddened with  $A_V = 4.5$ , and the X-ray data were corrected for absorption by  $N_{\text{H}} = 2 \times 10^{22} \text{ cm}^{-2}$ . Upper limits from the Fermi LAT ( $2 \times 10^{23} \text{ Hz}$ ) and from VERITAS<sup>29</sup> ( $10^{26} \text{ Hz}$ ) are also shown. The solid red curve is a blazar jet model<sup>30</sup> dominated by synchrotron emission, fitted to the spectral energy distribution of the brightest flares. On the low frequency side, the steep slope between the NIR and X-ray bands requires suppression of low-energy electrons, which would otherwise overproduce the NIR flux. This requires a particle-starved, magnetically dominated jet. On the high frequency side, the LAT (95%) and VERITAS (99%) upper limits require that the self-Compton component (red dashed line labelled ‘no pairs’) is suppressed by  $\gamma$ - $\gamma$  pair production, which limits the bulk Lorentz factor in the X-ray emitting region to be  $\Gamma \lesssim 20$ . The model includes a disk/corona component from the accretion disk (black dotted curve), but the flux is dominated at all frequencies by the synchrotron component from the jet. The blue curve shows the corresponding model in the low X-ray flux state. The kink in the X-ray spectrum in the low and intermediate flux states suggests that a possible additional component may be required; it would have to be very narrow, and its origin is unclear. Further details, including model parameters and two alternative models, are presented in Supplementary Information section 2.

variability can also be produced in a jet with substructure, in which case this constraint may underestimate the black hole mass. We obtain an independent constraint on the black hole mass from the relation between the mass of the central black hole,  $M_{\text{bh}}$ , and the luminosity of the galactic bulge,  $L_{\text{bulge}}$ . This gives an upper limit of  $\sim 2 \times 10^7 M_\odot$  (see Supplementary Information section 2.1 for details). We conclude that the dimensionless black hole mass,  $M_6$ , is likely to be between 1 and 20.

For a black hole of this size, the peak isotropic X-ray luminosity exceeds the Eddington luminosity,  $L_{\text{Edd}} = 1.3 \times 10^{44} M_6 \text{ erg s}^{-1}$ , by several orders of magnitude. If the radiation were truly isotropic, radiation pressure would halt accretion and the source would turn off. This contradiction provides strong evidence that the radiation pattern must be highly anisotropic, with a relativistic jet pointed towards us.

In addition to the X-ray observations discussed above, we obtained photometry in the uvw2, uvm2, uvw1, u, b, v, R, J, H and Ks bands with the Swift UVOT, LOAO, BOAO, TNG, UKIRT, CFHT and Maidanak Observatory telescopes (Supplementary Fig. 5). We used our broadband data set to construct spectral energy distributions at several key time periods in order to constrain models of the emission mechanism (Fig. 3). The spectral energy distributions show that the broadband energy spectrum is dominated by the X-ray band, which accounts for 50% of the total bolometric energy output in the high/flaring X-ray state. The optical counterpart of the transient X-ray source is not detected in optical or ultraviolet bands, but is detected strongly in

the NIR, indicating substantial extinction by dust in the host galaxy. We measure an extinction of  $A_V \approx 4.5$  (Supplementary Information section 1.2.3), which corresponds to a neutral hydrogen column density of  $N_{\text{H}} \approx 1 \times 10^{22} \text{ cm}^{-2}$  for the Galactic interstellar medium gas-to-dust ratio<sup>23</sup>; this is in rough agreement with the measured intrinsic X-ray absorption (Supplementary Fig. 11).

The spectral energy distribution constrains the possible emission mechanism. We assume that the NIR and X-ray photons originate in the same emission region, an assumption that is consistent with the NIR and X-ray spectral slopes. The optical-to-X-ray slope then requires a magnetically dominated, particle-starved jet. Although not shown here, we interpret the radio emission<sup>15</sup> as an external shock in the gas surrounding Swift J164449.3+573451. Details of our modelling are given in Supplementary Information sections 2.3–2.7.

This luminous, relativistic jet is probably powered by the tidal disruption of a star, which can explain the increase by four orders of magnitude in the X-ray flux from this supermassive black hole, the slow decay in flux following the initial outbursts, and the inferred mass accretion amounting to a substantial fraction of a solar mass (Supplementary Information section 2.2). It is not surprising for such an event to produce an X-ray jet<sup>6,24</sup>. If the accretion is powered by the tidal disruption of a star, we can estimate the jet beaming factor based on the expected statistics of tidal disruption events. The Swift BAT, with a field of view of  $\sim 4\pi/7$  sr and a duty cycle of  $\sim 75\%$ , has detected one such event in  $\sim 6$  years at a peak flux that would have been detectable to redshift  $z \approx 0.8$ . The all-sky rate of Swift J164449.3+573451-like events is therefore  $R_{4\pi} \approx 1 \text{ yr}^{-1}$ , with a 90% confidence interval<sup>25</sup> of  $0.08\text{--}3.9 \text{ yr}^{-1}$ . Taking into account the volume rate of tidal disruption events and the galaxy number density, and assuming that  $\sim 10\%$  of such events produce relativistic jets, we estimate that the fraction of tidal disruption events with jets pointed towards us must be  $\sim 10^{-3}$  (Supplementary Information section 2.9.1); a similar conclusion was obtained by the companion paper<sup>15</sup>. This jet solid angle can be achieved by a bulk Lorentz factor of  $\Gamma \approx 10\text{--}20$  or a jet opening angle of  $\theta_j \approx 5^\circ$ .

Our observations of Swift J164449.3+573451 provide a unique data set for studying the onset of jet activity from a supermassive black hole, and are consistent with a prediction that a low-density, magnetically dominated jet might be formed during the super-Eddington phase of a tidal disruption event<sup>6</sup>. However, little theoretical work has been published discussing observational signatures of the onset of such a jet. Instead, tidal disruption models have concentrated on emission from the stellar surface, the accretion disk and the surrounding medium: an X-ray or  $\gamma$ -ray thermal flare is expected from the surface of the star as it is crushed by the strong gravitational gradient of the black hole<sup>5,7</sup>, with peak luminosity of  $< 10^{44} \text{ erg s}^{-1}$  and a duration of tens of seconds; a phase of super-Eddington accretion of bound debris, accompanied by a wind that interacts with the surrounding medium<sup>6,26</sup>, will radiate in the ultraviolet–NIR<sup>6</sup> or X-ray<sup>26</sup> bands with luminosity  $\lesssim 10^{44} \text{ erg s}^{-1}$ , and at late times the bolometric luminosity from the accretion disk may undergo a steady decline that traces the mass accretion rate of post-disruption debris<sup>2,27,28</sup>,  $\frac{dM}{dt} \propto (t-t_0)^{-5/3}$ , where  $(t-t_0)$  is the time since the stellar disruption. Detailed multi-band light curve models of emission from the accretion disk in tidal disruption events suggest that the X-ray emission should be characterized by a broad, smooth X-ray light curve peaking at  $L_X \approx 3 \times 10^{44} \text{ erg s}^{-1}$  weeks to months after the stellar disruption for a  $10^6\text{--}10^7 M_\odot$  black hole<sup>26</sup>, in sharp contrast to our observations. The dramatic differences between these model predictions and our observations are probably due to the bright jet in Swift J164449.3+573451, which dominates the much fainter emission from the wind and disk. Long-term monitoring of Swift J164449.3+573451 will help to distinguish between competing models of this event, and will show whether emission from the jet follows the expected  $t^{-5/3}$  decay of the mass accretion rate from fallback of stellar debris.

Received 25 April; accepted 18 July 2011.

1. Rees, M. J. Tidal disruption of stars by black holes of  $10^6\text{--}10^8$  solar masses in nearby galaxies. *Nature* **333**, 523–528 (1988).
2. Evans, C. R. & Kochanek, C. S. The tidal disruption of a star by a massive black hole. *Astrophys. J.* **346**, L13–L16 (1989).
3. Ulmer, A. Flares from the tidal disruption of stars by massive black holes. *Astrophys. J.* **514**, 180–187 (1999).
4. Bogdanović, T., Eracleous, M., Mahadevan, S., Sigurdsson, S. & Laguna, P. Tidal disruption of a star by a black hole: observational signature. *Astrophys. J.* **610**, 707–721 (2004).
5. Guillochon, J., Ramirez-Ruiz, E., Rosswog, S. & Kasen, D. Three-dimensional simulations of tidally disrupted solar-type stars and the observational signatures of shock breakout. *Astrophys. J.* **705**, 844–853 (2009).
6. Strubbe, L. E. & Quataert, E. Optical flares from the tidal disruption of stars by massive black holes. *Mon. Not. R. Astron. Soc.* **400**, 2070–2084 (2009).
7. Brassart, M. & Luminet, J. Relativistic tidal compressions of a star by a massive black hole. *Astron. Astrophys.* **511**, A80 (2010).
8. Brandt, W. N., Pounds, K. A. & Fink, H. The unusual X-ray and optical properties of the ultrasoft active galactic nucleus Zwicky 159.034 (RE J1237+264). *Mon. Not. R. Astron. Soc.* **273**, L47–L52 (1995).
9. Komossa, S. & Bade, N. The giant X-ray outbursts in NGC 5905 and IC 3599: Follow-up observations and outburst scenarios. *Astron. Astrophys.* **343**, 775–787 (1999).
10. Donley, J. L., Brandt, W. N., Eracleous, M. & Boller, T. Large-amplitude X-ray outbursts from galactic nuclei: a systematic survey using ROSAT archival data. *Astron. J.* **124**, 1308–1321 (2002).
11. Esquej, P. et al. Candidate tidal disruption events from the XMM-Newton slew survey. *Astron. Astrophys.* **462**, L49–L52 (2007).
12. Gezari, S. et al. UV/optical detections of candidate tidal disruption events by GALEX and CFHTLS. *Astrophys. J.* **676**, 944–969 (2008).
13. Gezari, S. et al. Luminous thermal flares from quiescent supermassive black holes. *Astrophys. J.* **698**, 1367–1379 (2009).
14. Maksym, W. P., Ulmer, M. P. & Eracleous, M. A tidal disruption flare in A1689 from an archival X-ray survey of galaxy clusters. *Astrophys. J.* **722**, 1035–1050 (2010).
15. Zauderer, B. A. et al. The birth of a relativistic outflow in the unusual  $\gamma$ -ray transient Swift J164449.3+573451. *Nature* doi:10.1038/nature10366 (this issue).
16. Gehrels, N. et al. The Swift gamma-ray burst mission. *Astrophys. J.* **611**, 1005–1020 (2004).
17. Barthelmy, S. D. et al. The Burst Alert Telescope (BAT) on the SWIFT Midex mission. *Space Sci. Rev.* **120**, 143–164 (2005).
18. Burrows, D. N. et al. The Swift X-Ray Telescope. *Space Sci. Rev.* **120**, 165–195 (2005).
19. Goad, M. R. et al. Accurate early positions for Swift GRBs: enhancing X-ray positions with UVOT astrometry. *Astron. Astrophys.* **476**, 1401–1409 (2007).
20. Evans, P. A. et al. Methods and results of an automatic analysis of a complete sample of Swift-XRT observations of GRBs. *Mon. Not. R. Astron. Soc.* **397**, 1177–1201 (2009).
21. Levan, A. J. et al. An extremely luminous panchromatic outburst from the nucleus of a distant galaxy. *Science* **333**, 199–202 (2011).
22. Romano, P. et al. Two years of monitoring supergiant fast X-ray transients with Swift. *Mon. Not. R. Astron. Soc.* **410**, 1825–1836 (2011).
23. Bohlin, R. C., Savage, B. D. & Drake, J. F. A survey of interstellar H I from  $L\alpha$  absorption measurements. II. *Astrophys. J.* **224**, 132–142 (1978).
24. Grindlay, J. E. in *X-ray Timing 2003: Rossi and Beyond* (eds Kaaret, P., Lamb, F. K. & Swank, J. H.) 413–422 (Am. Inst. Phys. Conf. Ser., Vol. 714, 2004).
25. Kraft, R. P., Burrows, D. N. & Nousek, J. A. Determination of confidence limits for experiments with low numbers of counts. *Astrophys. J.* **374**, 344–355 (1991).
26. Lodato, G. & Rossi, E. M. Multiband light curves of tidal disruption events. *Mon. Not. R. Astron. Soc.* **410**, 359–367 (2011).
27. Phinney, E. S. in *The Center of the Galaxy* (ed. Morris, M.) 543–553 (IAU Symp., Vol. 136, 1989).
28. Lodato, G., King, A. R. & Pringle, J. E. Stellar disruption by a supermassive black hole: is the light curve really proportional to  $t^{-5/3}$ ? *Mon. Not. R. Astron. Soc.* **392**, 332–340 (2009).
29. Aliu, E. et al. VERITAS observations of the unusual extragalactic transient Swift J164449.3+573451. *Astrophys. J.* (in the press); preprint at <http://arXiv.org/abs/1107.1738>.
30. Ghisellini, G. & Tavecchio, F. Canonical high-power blazars. *Mon. Not. R. Astron. Soc.* **397**, 985–1002 (2009).

Supplementary Information is linked to the online version of the paper at [www.nature.com/nature](http://www.nature.com/nature).

**Acknowledgements** We acknowledge support from the following funding agencies: NASA, NSF and DOE (US); the UK Space Agency; ASI, INAF and INFN (Italy); the Autonomous Region of Sardinia; MEXT, KEK and JAXA (Japan); CRI/NRF/MEST (Korea); NSC and Academia Sinica (Taiwan); CEA/Irfu, IN2P3/CNRS and CNES (France); and the K. A. Wallenberg Foundation, the Swedish Research Council and the National Space Board (Sweden). We thank the Swift, Fermi and MAXI operation teams; and we thank A. Read for help with the most recent XMM slew data. We acknowledge the contribution of pre-publication upper limits by the VERITAS Collaboration. Finally, we acknowledge the use of public data from the Swift and Fermi data archives (<http://heasarc.nasa.gov/docs/swift/archive/> and <http://fermi.gsfc.nasa.gov/ssc/>, respectively), as well as data supplied by the UK Swift Science Data Centre at the University of Leicester. E.T. is a NASA Postdoctoral Fellow.

**Author Contributions** D.N.B., J.A.K. and M.E. composed the text, using inputs from the other co-authors. Theoretical interpretation was provided by G.G., B.Z., M.E. and P.M., with contributions by A.D.F., S. Campana and N.G.; J.A.K., V.M., K.L.P., J.P.O., P.R., S. Campana, A.P.B., V.D'E., P.E., P.A.E. and G.I. processed and analysed the Swift XRT data. T.S., J.R.C. and H.A.K. processed and analysed the Swift BAT data. Swift UVOT data were processed and analysed by A.A.B., M.M.C., S.T.H. and F.E.M. Ground-based optical/NIR data were obtained with the TNG, BOAO, LOAO, CFHT, UKIRT and Maidanak Observatory telescopes, and were provided, reduced and analysed by S. Covino, P.D'A., D.F., K.Y.H., M.I., H.D.J., Y.J., Y.-B.J., J.H.K., W.-K.P., H.-I.S., G.T., Y. Urata and L.A.A. Fermi LAT data analysis was performed by R.C., N.O., J.S.P. and E.T.; K.H., N.K., H.N., M.S., Y. Ueda and R.U. processed and analysed the MAXI data. A.D.F. provided liaison with the

VERITAS Collaboration. J.M.G. and P.G. provided analysis of ROSAT archival data, and J.P.O. provided analysis of archival XMM data. All authors discussed the results and commented on the manuscript.

**Author Information** Swift data are available from the NASA HEASARC (<http://swift.gsfc.nasa.gov/docs/swift/archive/>) or from mirror sites in the UK ([http://www.swift.ac.uk/swift\\_portal/archive.php](http://www.swift.ac.uk/swift_portal/archive.php)) and Italy (<http://swift.asdc.asi.it/>). Reprints and permissions information is available at [www.nature.com/reprints](http://www.nature.com/reprints). The authors declare no competing financial interests. Readers are welcome to comment on the online version of this article at [www.nature.com/nature](http://www.nature.com/nature). Correspondence and requests for materials should be addressed to D.N.B. ([burrows@astro.psu.edu](mailto:burrows@astro.psu.edu)).